Uniaxial Tension Behavior of FeNiCrCoAl and FeNiCrCoTi Complex Concentrated Alloys: A Molecular Dynamics Approach

Dheyaa F. Kadhim[1] 🟢 ⓘ • Zainalabden A. Ibrahim[2] • Falih H. Saddam Alazzawi[3]

Abstract

Complex concentrated alloys have been thoroughly examined for their excellent mechanical properties. In the present study, phase transitions and mechanisms of dislocation for FeNiCrCoAl and FeNiCrCoTi complex concentrated alloys were examined using classical molecular dynamics simulations under uniaxial tension. The (LAMMPS) code was used to simulate CCAs systems by using EAM potentials. The effect of strain rate change has been taken into account. The results show that at the early plastic stage, the main deformation behavior is the transition from FCC to HCP phase. Moreover, tensile characteristics are negatively affected by strain rate rise. At strain rate value of $1 \times 10^{10} \ s^{-1}$, for FeNiCrCoAl, elastic modulus and density are computed to be 83 Gpa and 7436 kg/m^3. Whereas, for FeNiCrCoTi, elastic modulus and density are calculated to be 46 Gpa and 7587 kg/m^3. It can be noticed that elasticity modulus of FeNiCrCoAl is two times greater than that of FeNiCrCoTi. In contrast, young modulus of complex concentrated alloys decreases succinctly when the strain rate increases to a value of $5 \times 10^{10} \ s^{-1}$. Under tensile deformation, the movement direction and impact on mechanical properties of the prevalent 1/6 <112> Shockley partial dislocations are analyzed.

Keywords— Complex concentrated alloys, Tension properties, Molecular dynamics.

1 Introduction

Comprising at least five constituent elements, complex concentrated alloys (CCAs), also called high-entropy alloys, are a distinct class of alloys that set them apart from normal alloys. This causes a significant increase in configurational entropy and combining in the solid as well as the liquid state. Among the exceptional mechanical properties are high strength, superior ductility, outstanding wear resistance, and corrosion resistance (Rao et al., 2024). (Mu et al., 2023) at temperatures between 1370 and 1430 degrees Celsius, examined the wettability of the liquid Ti$_{0.2}$FeCoCrNi CCA on the (HfZrNbTiTa) high-entropy ceramic (HEC). The dissolved HEC introduced atoms of Hf and Zr, and their adhesion across the triplet line aided in the reduction of the angle. In the meantime, the HEC experienced a phase shift with the same lattice structure. Recently, many CCA systems have been used; however, most research have concentrated on the characteristics and microstructure of the CoCrFeNiAl CCAs system. Based on recent investigations, CCAs have been found to have superior qualities than standard alloys, including superior thermal stability, outstanding fatigue, wear, enhanced hardness, and extraordinary capabilities at high and cryogenic temperatures. Because of these characteristics, CCAs are good candidates to meet the strict specifications needed for specialized, high-stakes applications, particularly in the turbine, nuclear, and aircraft industries. One of the most widely used CCA today is Al$_x$CoCrFeNi, which was among the first to be studied. The mechanical properties of CoCrFeNiAl CCA and how various elemental concentrations affect those properties. In addition, the CCAs have many exceptional mechanical properties, high strength, corrosion resistance, and excellent performance at both lowered and elevated temperature (Ren et al., 2022).

Dheyaa F. Kadhim
dheyaa.kadhim@utq.edu.iq

Zainalabden A. Ibrahim
zainalabden.A @utq.edu.iq

Falih H. Saddam Alazzawi
Alazzawi.eng1973@gmail.com

[1] Department of Studies and Planning, University of Thi-Qar, Nasiriyah, 64001, Iraq
[2] Department of Bureau Affairs, University of Thi-Qar, Nasiriyah, 64001, Iraq
[3] Department of Mechanical Engineering, University of Thi-Qar, Nasiriyah, 64001, Iraq

In a single-crystal FeCoNiCrMn CCA (Alabd Alhafez et al., 2019) used MD to examine the mechanical behavior of nano-indentation. It was discovered that the alloy produces longer and more concentrated dislocations than pure Ni does. Amorphization does not occur during the deformation process. Using MD modeling (Fang et al., 2019) examined a heteroclinic hexagonal array (CCA) made up of FCC and HCP phases. For the tensile alloy, they indicated a potent interfacial hardening process. The alloy has excellent ductility and high strength. The mechanical characteristics of FeCrNiCoMn CCAs with various grain sizes were investigated by (Otto et al., 2013). They discovered that as grain size decreases, the alloy's yield strength rises. As temperature rises during the deformation process, the impact of fine-grain strengthening decreases. By using MD, (Ruestes & Farkas, 2022) examined the FeNiCrCoCu HEA nano-indentation's plastic deformation mechanism. They discovered that dislocation motion primarily affects the deformation. Dislocation linkages that emerge during the deformation process cause the material to become harder. The structural evolution of a CCA via MD was examined by HE. They discovered that there are two variables that contribute to stacking fault strengthening. Two causes are the creation of the antiphase domain border and the variation in stacking fault energy between the CCA matrix and its precipitate phase (J. Li et al., 2020). In order to understand how strain, strain rate, and temperature affect the mechanistic properties, (Raturi et al., 2021) undertook a mechanistic viewpoint on the kinetics of plastic deformation in an FCC CCA. They recommended that in order to comprehend the activation processes of dislocations, multi-length and time-scale simulations be used, together with theoretical studies to create a grasp of the dislocation structure. The CoCrFeNiAl alloy was selected for this work because it has been the subject of substantial experimental investigation. On the other hand, little research has been done on the nanoscale deformation mechanisms of Al_xCoCrFeNi CCA. To the best of our knowledge, however, the nanoscale phase change and tensile mechanisms of CoCrFeNiAl have not been studied. Molecular Dynamics (MD) is a useful tool for exploring the microstructural and mechanical properties to get a comprehension of the deformation characteristics of materials at the nanoscale. The approach is to represent the potential-energy hypersurface of a material using a set of parametric functions. A precise interatomic potential is necessary for the simulations. The best interatomic-potential model for CoCrFeNiAl CCA is the embedded atom method (EAM), which uses the same mathematical formalization to display different elements within different structures (Qin et al., 2019).

In the current work, the phase transformation and microstructural evolution of nanocrystalline FeNiCrCoAl and FeNiCrCoTi CCAs were investigated under tension using MD simulation; the relationship between the plastic deformation behavior and micromechanics for FeNiCrCoAl and FeNiCrCoTi CCAs was studied; the microstructural evolution for the phase transformation from FCC to HCP was disclosed. In order to examine the crystal structure, the radial distribution functions (RDF) were computed in order to determine and characterize the local atomic structures.

2 Methodology

2.1 Simulation

The (LAMMPS) simulator is used to simulate CCAs systems (Plimpton, 1995). The first step is to practice relaxation. The solid solution FeNiCrCoAl and FeNiCrCoTi CCAs system can be sent to the NVE ensemble at $300K$ for $160ps$ (picoseconds) in order to achieve the relaxation. Alternatively, the isobaric-isothermal ensemble at $300K$ for $200ps$ can be utilized. The relaxing process is finished once equilibrium is achieved. This is followed by applying strain rates of 1×10^{10}, 3×10^{10} and 5×10^{10} s^{-1} along the x-direction. Tension loads are applied with a time step of one femtosecond (fs) along the x-direction until sample reach failure stage. The Verlet velocity method is used in conjunction with periodic boundary conditions (Verlet, 1967).

2.2 Interatomic potential

The EAM potentials employed to simulate the metallic system since it has been widely used for CCAs to precisely mimic the material's structural characteristics since it can illustrate a variety of components with different structural modifications that adhere to the same mathematical foundation. In the current research, we applied an EAM potential function for FeNiCrCoAl and FeNiCrCoTi CCAs that was presented by (Farkas & Caro, 2020) and (Liang et al., 2023), respectively.

2.3 Lattice setup

Cr (red), Al (green), Ni (blue), Fe (violet), and Ti (brown) and Co (yellow). Atoms to be scattered in an FCC lattice of $(14a, 14a, 14a)$ nm^3 as depicted in Figure 1, lattice constants for FeNiCrCoAl, $a = 0.357nm$ and for FeNiCrCoTi, $a = 0.356nm$. Periodic boundary conditions apply to all directions. Visualization software (OVITO)

(Stukowski, 2010), Common Neighbor Analysis (CNA) (Honeycutt & Andersen, 1987) and DXA algorithm (Stukowski & Albe, 2010) were utilized for post-processing of molecular trajectories. After that, the structure is started at $300K$ in a (NPT ensemble) which means constant (number of atoms, pressure and temperature) and permitted to stabilize for an additional $91ps$. After that, the CCA is repeatedly quenched under the Nóse-Hoover for $10ps$. The final step in quenching under the (NVE) ensemble which means constant (number of atoms, volume and energy) is to give the structure $15ps$ to equilibrate.
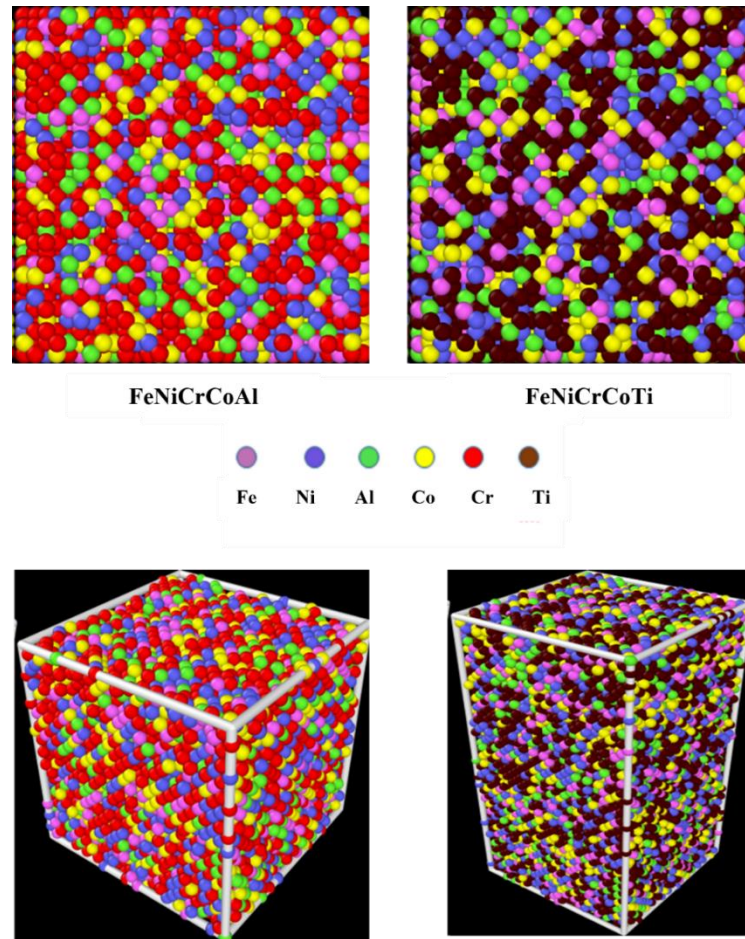

Figure 1: Represents the 3D MD model for FeNiCrCoAl and FeNiCrCoTi alloy

3   Results and discussions

3.1   Structural analysis

Studies on the experimental characteristics of alloys, such as the CoCrFeNiAl complex concentrated alloys, have been conducted. Reports on the qualities of computational tension, however, are scarce. Figure 2 displays the CNA results for the alloy that is not deformed. We find that the FCC (63%) and disordered coordination (37%) which comprise the remaining phases—hexagonal close packed (HCP), at roughly 12.38%, and BCC, at 9.2%—are barely slightly present. Consistent with experimental results (Liang et al., 2023), the typical FCC recognition of a lattice is given by spikes in alongside nearest neighbor atoms spaced at prescribed intervals. By averaging all atom pairs, this is repeated to yield the structural pair function, which is visible in Figure 2. Allowing us to forecast the deformation mechanisms through predictive analyses that were previously limited to experimental research. Many researchers have reported that CoCrFeNiAl compose of FCC structure (Bhattacharjee et al., 2018; Q. Wang et al., 2018; Wu et al., 2020). It is thought that slow effects and entropy, which reduce the Gibbs energy, are the reasons why such alloys formed a single solution instead of intermetallic phases. Several studies have shown that CoCrFeNiAl is composed of a single FCC phase. Moreover, FeNiCrCoTi alloy possesses FCC crystal structure (Q. Li et al., 2021).

3.2   Room-temperature physical properties

Figure 3 illustrates the stress-strain curves for FeNiCrCoAl and FeNiCrCoTi CCAs at strain rate of $1 \times 10^{10} \ s^{-1}$ and 301K. It is observed that there is a limit to the elastic stress strain at 3% strain, above which results in yield and subsequently plastic deformation. It has been observed that fracture strain for CoCrFeNiAl CCAs increases with increasing temperature (Kim et al., 2022). However, the higher the temperature, the slower the stress
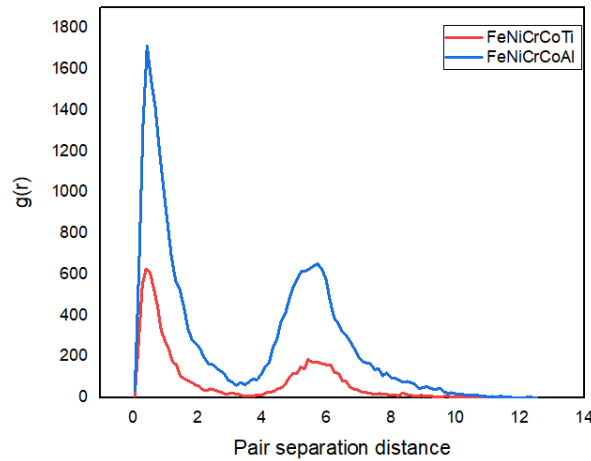

Figure 2 The structural pair function for both CCAs

declines from a yield plateau following yield stress. It is easy to understand from an energy perspective that at greater temperatures, the motion of the atoms will be too hard to mobilize, which consequently reduces the structural stability of the CCAs. It is evident that the CCA strain is mostly distributed throughout the CCAs zone at low temperatures because of the CCAs very localized distortion. Annealing increases the yielding strength of CoCrFeNiAl CCA to $870 \ MPa$ and $1060 \ MPa$, respectively, according to experimental results by (Q. Wang et al., 2018) This is a solid indication that the partial recrystallization process in this alloy produced an excellent balance between strength and flexibility. Another feature of CoCrFeNiAl CCA is that it includes the FCC and BCC phases. It suggests that this alloy composition is likely to split into multiple phases upon undergoing the appropriate annealing treatment. This offers a substantial chance to improve the strength by adjusting the precipitate characteristics because of their propensity to act as barriers to dislocation motion. The density and elasticity modulus at $300K$ are given in Table 1 and are derived from the stress / strain curve's linear slope in Figure 3. For FeNiCrCoAl, ρ and E determined to be $83 \ Gpa$ and $7436 \ kg/m^3$. Whereas, for FeNiCrCoTi, ρ and E determined to be $46 \ Gpa$ and $7587 \ kg/m^3$. It can be noticed that E for FeNiCrCoAl is greater than that of FeNiCrCoTi, in order of two times and this can be attributed to the Al content (T. Yang et al., 2015).

Table 1 Estimates from molecular simulations for (E) and (ρ) at 301 K.

Property (MD)	FeNiCrCoAl	FeNiCrCoTi
ρ (kg/m3)	7436	7587
E (GPa)	83	46

3.3   The Effect of Strain Rate

Through the analysis of the FeNiCrCoAl and FeNiCrCoTi CCAs stress-strain relationship at $300K$ and strain rates of $3x10^{10}$ and $5x10^{10} \ s^{-1}$. There has been a focus on the effects of rate of strain on the CCAs tensile characteristics. Figure 4 shows that, at the same temperature, the elastic modulus of the alloy remains largely unaffected whereas the yield stress and strain of CCAs increase as the strain rate does. In order to increase the free volume, one can increase the strain rate. However, the time required to rearrange atom mobility will be significantly shortened at higher strain rates. A linear elastic technique is used in the initial stage. The tension reaches its maximum as the deformation progresses and then abruptly decreases. Persistent plastic deformation at low tension occurs in the third stage until the entire structure breaks (Liu et al., 2020). Consequently, during

deformation, the strength of material will rise and atom mobility will become more problematic since less volume is available, which effects atom migration throughout deforming process.
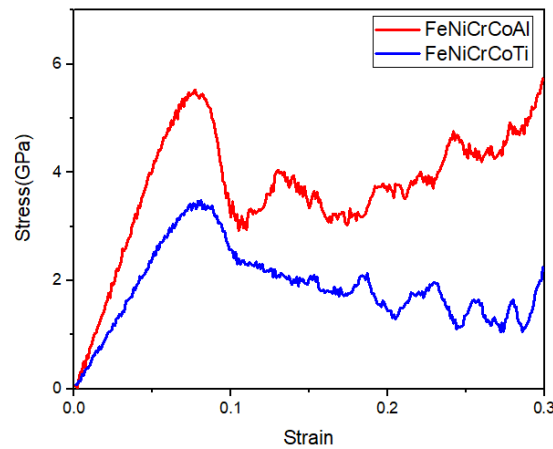

Figure 3: Stress-strain curves of FeNiCrCoAl and FeNiCrCoTi CCAs at 1x10^{10} strain rate

The CoCrFeNiAl CCA elasticity modulus rises from 83 to 86 Gpa when the strain rate raised from 1×10^{10} to $3 \times 10^{10} \ s^{-1}$. Whereas, the Young's modulus decreases to 81 Gpa at strain rate of $5 \times 10^{10} \ s^{-1}$. On the other hand, Young's modulus of the FeNiCrCoTi raised from 46 to 48 Gpa during strain rate rising from 1×10^{10} to $3 \times 10^{10} \ s^{-1}$. Whereas, the Young's modulus decreases to 51 Gpa at strain rate of $5 \times 10^{10} \ s^{-1}$. Furthermore, the elevation in strain rate has a stronger impact on the yield strength and E of CCAs with higher Al concentrations. Because of the length and time scale constraints, MD simulations employ higher strain rates of $10^{10} \ s^{-1}$ to generate a forecast within a realistic computed time (Tsai et al., 2015). As a result, the yield strength may be greater than the experimental value. Nonetheless, the CCAs deformation shown in our study are consistent with those observed in experiments at high strain rates. (L. Wang et al., 2018) investigated dynamic loading on Al$_{0.6}$CoCrFeNi CCAs and they found that increasing the strain rate had no appreciable impact.
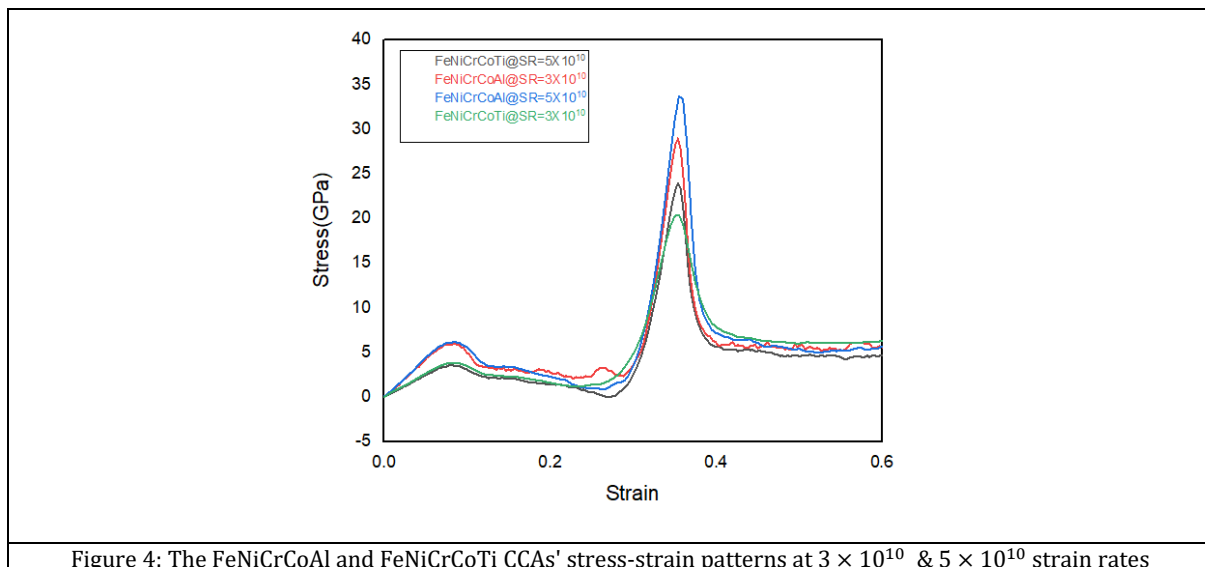

Figure 4: The FeNiCrCoAl and FeNiCrCoTi CCAs' stress-strain patterns at 3×10^{10} & 5×10^{10} strain rates

3.4   Mechanisms of dislocation

Different dislocations observed tension loading on FeNiCrCoAl and FeNiCrCoTi are shown in Figure 5. CCAs at $300K$ and a strain rate of $1 \times 10^{10} \ s^{-1}$. To recognize types of a dislocation, they are colored differently: A green refers to perfect dislocation, a blue for a Shockley, a magenta for a Hirth, a cyan a stair-rod, yellow for Frank, and a red for others. From Figure 5, for FeNiCrCoAl, Undoubtedly, since a Shockley-type dislocation is simpler to

originate and sliding in a (111) face than a (010) face, Shockley and Hirth have the upper hand (F. Yang et al., 2022). Whereas, FeNiCrCoTi, Shockley and stair rods prevail with no traces for Hirth and this in line with Liu et al. (Liu et al., 2020) They discovered that dislocation transforms the grain boundary and that the grain boundary influences dislocation movement. The strength in a CCA may be increasing mostly because of this deformation mechanism. According to experimental findings, stacking faults arise and disappear in a single phase as a result of the mobility of Shockley partials during deformation (T. Yang et al., 2017). Therefore, the Shockley in the CCA fits the strain during deforming and reduce storage. Besides, MD examined a tensile and scratching CCA in the study of Fan et al. (Fan et al., 2022) Under uniaxial tensile stress, they discovered that the HEA exhibits substantial anisotropy. In the tensile instance, stacking defects are transported via Shockley dislocation, which is deeper into the substrate than in the scratching scenario. An increase in strain hardening is apparently restricted when a large number of Shockley dislocations are present. The dislocation density (ρ_d) variation at $300K$ with strain. The dislocation number in an alloy can be calculated using the formula $d = D_L/V$, where D_L is the dislocation line's total length and V is the simulation cell's volume. Density begins at $5.4 \times 10^{17} \ m^{-2}$ for FeNiCrCoAl CCA and $4.3 \times 10^{17} \ m^{-2}$ FeNiCrCoTi CCA. As a result, it can be observed that at $300K$, plastic deformation removes dislocations in both CCAs. In contrast, strain hardening occurs at greater strain rates as a result of an increase in dislocation density brought on by the dislocations' constrained motion, which leads to the creation of defects such as additional vacancies and dislocations. It is noteworthy that the dislocation density rises with strain indicates a positive correlation between dislocation formation and deformation during plasticity (Qi, Xu, et al., 2021).
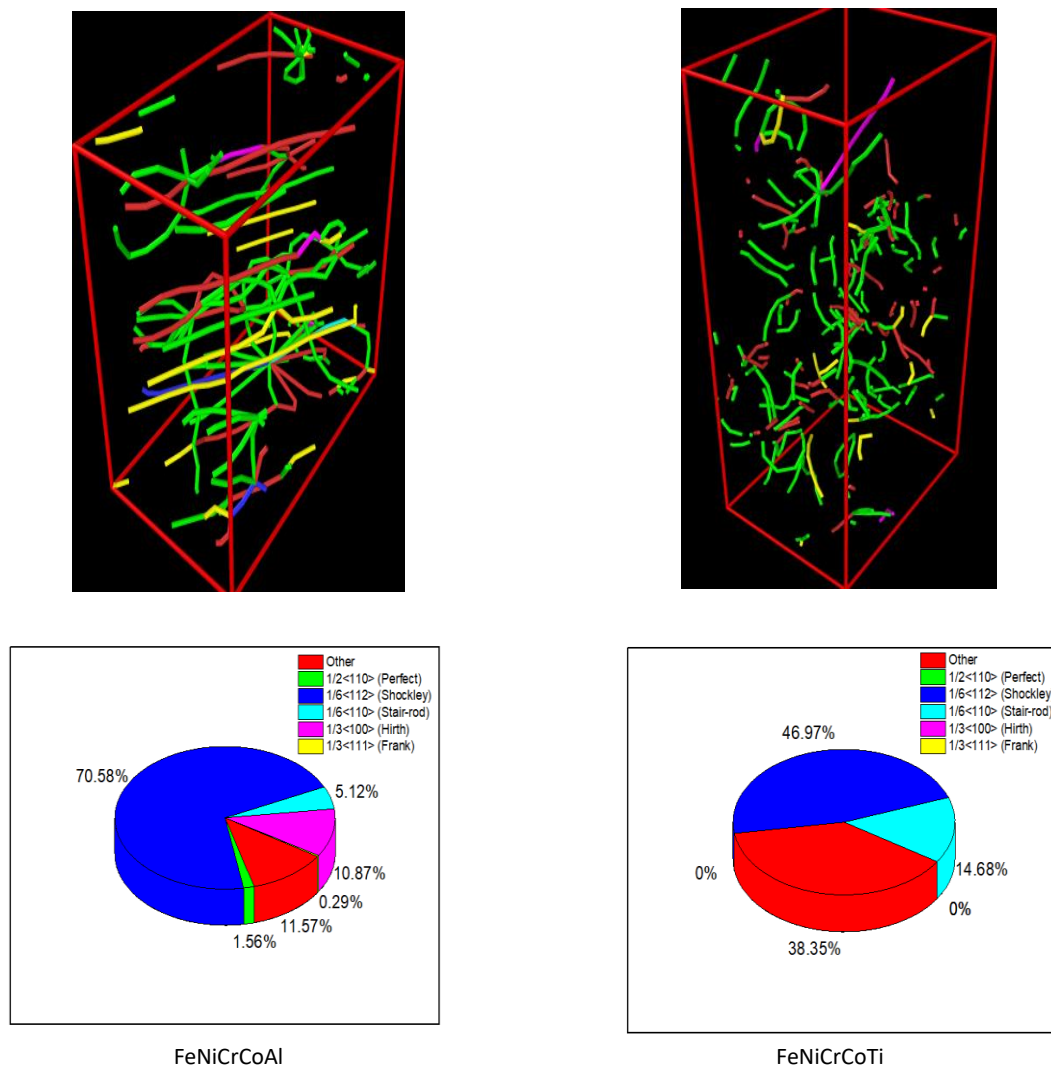

FeNiCrCoAl   FeNiCrCoTi

Figure 5: Dislocation progression of both CCAs at 300K

3.5 Phase Transformations

Figure 6 shows diagram illustrating the change from FCC to HCP. For the deformed FeNiCrCoAl and FeNiCrCoTi CCAs alloy at $300K$, As seen in Figure 6, CNA sheds light on deformation mechanisms such as twin boundaries (TBs) and intrinsic and extrinsic stacking faults (SF). As can be seen, slippage had a major role in controlling the plastic stage, and stacking faults were important to the process. The emergence of stacking fault networks led to the discovery of the behavior of stress fluctuation. A frequent planar defect that arises during the deformation of face-centered cubic (FCC) metals is called an intrinsic stacking fault. When an inherent stacking fault is introduced long the closed-packed (111) planes, the FCC alloys naturally stack in the ABC ABC AB arrangement, but the stacking pattern becomes ABCBCABC. The otherwise flawless stacking appears to have been disturbed by the removal of one closed plane, A in this instance. Obtaining the standardized stacking fault energy for the modeled high entropy alloy was deemed reasonable, given it is located in an FCC phase (Fan et al., 2022), When the model starts sliding under tension, there is friction between the nearby HCP ISFs; this friction, in contrast to friction in metal alone, is extremely noticeable due to the difference in component radii. The quantity of FCC atoms decreases as the number of HCP and other atoms rises. It implies an increased conversion of SFs into HCP structures (Luo et al., 2021). Partial dislocation interactions also produce additional barriers that contribute to rise hardness. Moreover, imperfect dislocation components work together to form a body flaw in the stacking faults pattern. An additional Shockley incomplete dislocation on the neighboring plane generates the extrinsic stacking fault (ESF). The separation of Shockley partial dislocations determines the varying times at which intrinsic SFs emerge. The Shockley partial dislocations dissolve further into the crystal lattice as strain increases; this action lengthens the intrinsic SFs (Qi, Zhao, et al., 2021). The twinned zone is divided into two twin limits, according to ESF. It is important to remember that the FCC structure in the simulation does not instantly transition into the HCP phase. Owing to intrinsic stacking faults (ISF) generally low energy, the transformation needs an intermediate ISF product. ISF uses less energy than other materials, which helps it produce HCP. This observation suggests that phase change is no longer the beginning point of deformation (Qi, Xu, et al., 2021). It is commonly accepted that in nanocrystalline materials, higher strain rates encourage deformation twinning (Zhu et al., 2012).

4 Conclusion

Using classical molecular dynamics computations, two FeNiCrCoAl and FeNiCrCoTi high-entropy alloys either Al or Ti were studied. We investigated how strain rate ($1 \times 10^{10}\ s^{-1}$, $3 \times 10^{10}\ s^{-1}$ and $5 \times 10^{10}\ s^{-1}$) affected the tensile characteristics of both CCAs. It was concluded that when the strain rate raised, the elasticity modulus of both CCAs decreased, which in agreement with experimental results. At strain rate of $1 \times 10^{10}\ s^{-1}$, for FeNiCrCoAl CCA, it is evident that the Shockley and Hirth outweigh all other types. Whereas, FeNiCrCoTi CCA, Shockley and stair rods prevail with no traces for Hirth. Shockley fractional dislocations migrate during the early stages of deformation, causing stacking errors to occur and vanish in a single step. The Shockley in the structure absorbs the force as the CCA deforms. This finding implies that the capacity to increase When strain hardening gets higher, CCA strength is drastically impeded when Shockley dislocations are heavily existent.

Limitations and directions for future research are as follow:
1. Simulations need prolonged time to process.
2. Super computer is required to run simulation with higher number of atoms.
3. more parameters can be changed such as temperature and investigating its effects on both alloys' behavior during tension.
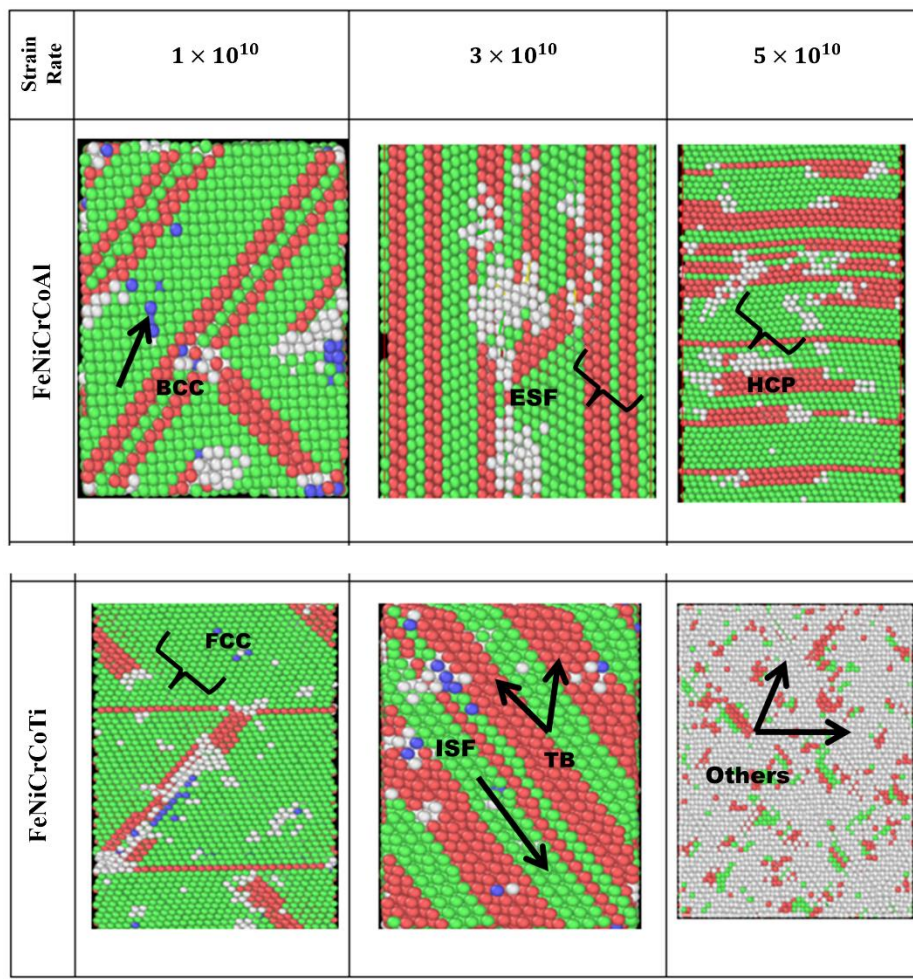
Figure 6: Atomic configurations and related schematics for phase transitions from FCC to HCP at 300 K

References

Alabd Alhafez, I., Ruestes, C. J., Bringa, E. M., & Urbassek, H. M. (2019). Nanoindentation into a high-entropy alloy – An atomistic study. *Journal of Alloys and Compounds*, *803*, 618–624. https://doi.org/10.1016/j.jallcom.2019.06.277

Bhattacharjee, T., Wani, I. S., Sheikh, S., Clark, I. T., Okawa, T., Guo, S., Bhattacharjee, P. P., & Tsuji, N. (2018). Simultaneous Strength-Ductility Enhancement of a Nano-Lamellar AlCoCrFeNi2.1 Eutectic High Entropy Alloy by Cryo-Rolling and Annealing. *Scientific Reports*, *8*(1), 3276. https://doi.org/10.1038/s41598-018-21385-y

Fan, P., Katiyar, N. K., Zhou, X., & Goel, S. (2022). Uniaxial pulling and nano-scratching of a newly synthesized high entropy alloy. *APL Materials*, *10*(11). https://doi.org/10.1063/5.0128135

Fang, Q., Chen, Y., Li, J., Jiang, C., Liu, B., Liu, Y., & Liaw, P. K. (2019). Probing the phase transformation and dislocation evolution in dual-phase high-entropy alloys. *International Journal of Plasticity*, *114*, 161–173. https://doi.org/10.1016/j.ijplas.2018.10.014

Farkas, D., & Caro, A. (2020). Model interatomic potentials for Fe–Ni–Cr–Co–Al high-entropy alloys. *Journal of Materials Research*, *35*(22), 3031–3040. https://doi.org/10.1557/jmr.2020.294

Honeycutt, J. Dana., & Andersen, H. C. (1987). Molecular dynamics study of melting and freezing of small Lennard-Jones clusters. *The Journal of Physical Chemistry*, *91*(19), 4950–4963. https://doi.org/10.1021/j100303a014

Kim, J.-K., Kim, J. H., Park, H., Kim, J.-S., Yang, G., Kim, R., Song, T., Suh, D.-W., & Kim, J. (2022). Temperature-dependent universal dislocation structures and transition of plasticity enhancing mechanisms of the Fe40Mn40Co10Cr10 high entropy alloy. *International Journal of Plasticity*, *148*, 103148. https://doi.org/10.1016/j.ijplas.2021.103148

Li, J., Chen, H., Fang, Q., Jiang, C., Liu, Y., & Liaw, P. K. (2020). Unraveling the dislocation–precipitate interactions in high-entropy alloys. *International Journal of Plasticity*, *133*, 102819. https://doi.org/10.1016/j.ijplas.2020.102819

Li, Q., Bao, X., Zhao, S., Zhu, Y., Lan, Y., Feng, X., & Zhang, Q. (2021). The Influence of AlFeNiCrCoTi High-Entropy Alloy on Microstructure, Mechanical Properties and Tribological Behaviors of Aluminum Matrix Composites. *International Journal of Metalcasting*, *15*(1), 281–291. https://doi.org/10.1007/s40962-020-00462-x

Liang, A., Goodelman, D. C., Hodge, A. M., Farkas, D., & Branicio, P. S. (2023). CoFeNiTi and CrFeNiTi high entropy alloy thin films microstructure formation. *Acta Materialia*, *257*, 119163. https://doi.org/10.1016/j.actamat.2023.119163

Liu, C., Yang, Y., & Xia, Z. (2020). Deformation mechanism in Al (0.1) CoCrFeNi Sigma3(111)[1$\bar{1}$0] high entropy alloys – molecular dynamics simulations. *RSC Advances*, *10*(46), 27688–27696. https://doi.org/10.1039/D0RA01885F

Luo, G., Li, L., Fang, Q., Li, J., Tian, Y., Liu, Y., Liu, B., Peng, J., & Liaw, P. K. (2021). Microstructural evolution and mechanical properties of FeCoCrNiCu high entropy alloys: a microstructure-based constitutive model and a molecular dynamics simulation study. *Applied Mathematics and Mechanics*, *42*(8), 1109–1122. https://doi.org/10.1007/s10483-021-2756-9

Mu, R., Wang, Y., Niu, S., Sun, K., & Yang, Z. (2023). Wetting of FeCoCrNiTi0.2 high entropy alloy on the (HfZrTiTaNb)C high entropy ceramic. *Journal of the European Ceramic Society*, *43*(16), 7263–7272. https://doi.org/10.1016/j.jeurceramsoc.2023.07.065

Otto, F., Dlouhý, A., Somsen, Ch., Bei, H., Eggeler, G., & George, E. P. (2013). The influences of temperature and microstructure on the tensile properties of a CoCrFeMnNi high-entropy alloy. *Acta Materialia*, *61*(15), 5743–5755. https://doi.org/10.1016/j.actamat.2013.06.018

Plimpton, S. (1995). Fast Parallel Algorithms for Short-Range Molecular Dynamics. *Journal of Computational Physics*, *117*(1), 1–19. https://doi.org/10.1006/jcph.1995.1039

Qi, Y., Xu, H., He, T., Wang, M., & Feng, M. (2021). Atomistic simulation of deformation behaviors polycrystalline CoCrFeMnNi high-entropy alloy under uniaxial loading. *International Journal of Refractory Metals and Hard Materials*, *95*, 105415. https://doi.org/10.1016/j.ijrmhm.2020.105415

Qi, Y., Zhao, M., & Feng, M. (2021). Molecular simulation of microstructure evolution and plastic deformation of nanocrystalline CoCrFeMnNi high-entropy alloy under tension and compression. *Journal of Alloys and Compounds*, *851*, 156923. https://doi.org/10.1016/j.jallcom.2020.156923

Qin, G., Xue, W., Chen, R., Zheng, H., Wang, L., Su, Y., Ding, H., Guo, J., & Fu, H. (2019). Grain refinement and FCC phase formation in AlCoCrFeNi high entropy alloys by the addition of carbon. *Materialia*, *6*, 100259. https://doi.org/10.1016/j.mtla.2019.100259

Rao, K. R., Dewangan, S. K., Seikh, A. H., Sinha, S. K., & Ahn, B. (2024). Microstructure and Mechanical Characteristics of AlCoCrFeNi-Based ODS High-Entropy Alloys Consolidated by Vacuum Hot Pressing. *Metals and Materials International*, *30*(3), 726–734. https://doi.org/10.1007/s12540-023-01530-7

Raturi, A., Biswas, K., & Gurao, N. P. (2021). A mechanistic perspective on the kinetics of plastic deformation in FCC High Entropy Alloys: Effect of strain, strain rate and temperature. *Scripta Materialia*, *197*, 113809. https://doi.org/10.1016/j.scriptamat.2021.113809

Ren, H., Chen, R. R., Gao, X. F., Liu, T., Qin, G., Wu, S. P., & Guo, J. J. (2022). Phase formation and mechanical features in (AlCoCrFeNi)100-Hf high-entropy alloys: The role of Hf. *Materials Science and Engineering: A*, *858*, 144156. https://doi.org/10.1016/j.msea.2022.144156

Ruestes, C. J., & Farkas, D. (2022). Dislocation emission and propagation under a nano-indenter in a model high entropy alloy. *Computational Materials Science*, *205*, 111218. https://doi.org/10.1016/j.commatsci.2022.111218

Stukowski, A. (2010). Visualization and analysis of atomistic simulation data with OVITO–the Open Visualization Tool. *Modelling and Simulation in Materials Science and Engineering*, *18*(1), 015012. https://doi.org/10.1088/0965-0393/18/1/015012

Stukowski, A., & Albe, K. (2010). Extracting dislocations and non-dislocation crystal defects from atomistic simulation data. *Modelling and Simulation in Materials Science and Engineering*, *18*(8), 085001. https://doi.org/10.1088/0965-0393/18/8/085001

Tsai, C.-W., Tsai, M.-H., Tsai, K.-Y., Chang, S.-Y., Yeh, J.-W., & Yeh, A.-C. (2015). Microstructure and tensile properties of Al 0.5 CoCrCuFeNi alloys produced by simple rolling and annealing. *Materials Science and Technology*, *31*(10), 1178–1183. https://doi.org/10.1179/1743284714Y.0000000754

Verlet, L. (1967). Computer "Experiments" on Classical Fluids. I. Thermodynamical Properties of Lennard-Jones Molecules. *Physical Review*, *159*(1), 98–103. https://doi.org/10.1103/PhysRev.159.98

Wang, L., Qiao, J. W., Ma, S. G., Jiao, Z. M., Zhang, T. W., Chen, G., Zhao, D., Zhang, Y., & Wang, Z. H. (2018). Mechanical response and deformation behavior of Al0.6CoCrFeNi high-entropy alloys upon dynamic loading. *Materials Science and Engineering: A*, *727*, 208–213. https://doi.org/10.1016/j.msea.2018.05.001

Wang, Q., Lu, Y., Yu, Q., & Zhang, Z. (2018). The Exceptional Strong Face-centered Cubic Phase and Semi-coherent Phase Boundary in a Eutectic Dual-phase High Entropy Alloy AlCoCrFeNi. *Scientific Reports*, *8*(1), 14910. https://doi.org/10.1038/s41598-018-33330-0

Wu, J., Yang, Z., Xian, J., Gao, X., Lin, D., & Song, H. (2020). Structural and Thermodynamic Properties of the High-Entropy Alloy AlCoCrFeNi Based on First-Principles Calculations. *Frontiers in Materials*, *7*. https://doi.org/10.3389/fmats.2020.590143

Yang, F., Cai, J., Zhang, Y., & Lin, J. (2022). Temperature and Crystalline Orientation-Dependent Plastic Deformation of FeNiCrCoMn High-Entropy Alloy by Molecular Dynamics Simulation. *Metals*, *12*(12), 2138. https://doi.org/10.3390/met12122138

Yang, T., Tang, Z., Xie, X., Carroll, R., Wang, G., Wang, Y., Dahmen, K. A., Liaw, P. K., & Zhang, Y. (2017). Deformation mechanisms of Al0.1CoCrFeNi at elevated temperatures. *Materials Science and Engineering: A*, *684*, 552–558. https://doi.org/10.1016/j.msea.2016.12.110

Yang, T., Xia, S., Liu, S., Wang, C., Liu, S., Zhang, Y., Xue, J., Yan, S., & Wang, Y. (2015). Effects of AL addition on microstructure and mechanical properties of Al CoCrFeNi High-entropy alloy. *Materials Science and Engineering: A*, *648*, 15–22. https://doi.org/10.1016/j.msea.2015.09.034

Zhu, Y. T., Liao, X. Z., & Wu, X. L. (2012). Deformation twinning in nanocrystalline materials. *Progress in Materials Science*, *57*(1), 1–62. https://doi.org/10.1016/j.pmatsci.2011.05.001